7 Laser Isotope Separation with Shaped Light

Andrew Forbes and Lourens Botha†

CONTENTS

7.1 INTRODUCTION

Laser-induced chemistry is an exciting and expanding field, which has led to commercial spin-off opportunities, such as the separation of isotopes of a given atom by means of selective laser-induced dissociation of a molecular structure containing those isotopes. This process, sometimes referred to as isotope enrichment, or just plain *enrichment*, is often the result of the molecule absorbing multiple photons, usually from an intense laser source. When a molecule is highly excited, it absorbs laser radiation by resonance, leading to dissociation of the weakest bonds. When the absorbed energy exceeds the dissociation energy of the weakest bond, the molecule undergoes decomposition. The trick is to make the absorption *selective*, so that only those molecules containing a particular isotope undergo this decomposition. One

usually chooses the initial molecule so that after decomposition, the final molecule differs from the original in some chemical or physical way. For example, one might choose the initial molecule to be in gas form, which forms solid decomposition products. The isotopes of a given atom are then separated by conventional techniques, which, in our example, would be a phase separation (separating the solids from the gases).

Since the suggestion first appeared that the absorption of laser radiation and the subsequent decomposition of molecules could be isotopically selective, a good deal of work has gone into demonstrating this. The focus has been on several isotopes of commercial interest, with somewhat divergent absorption properties, and consequently multiple-laser systems have been investigated as the source of the radiation, covering the spectral range from the vacuum ultraviolet to the far infrared. Infrared lasers have, for example, been used in investigating the enrichment of uranium for nuclear fuel, and the separation of ^{12}C isotopes for better thermal management in electronic circuitry. Although laser-induced chemistry and laser isotope separation have received much attention in the past, very little of the initial expectations have been realized commercially. The obstacles to successful commercialization to date have been as follows:

i. The cost of producing laser photons (or laser energy)
ii. The utilization of these photons on an industrial scale

The first obstacle has more or less been removed in the case of CO_2 laser photons: running and capital costs have decreased over the past decade to a level that the industrial applications of infrared selective isotope separation have become feasible and economically viable (although photons are still very expensive as compared to electrical energy). This reduction in cost is mostly due to a maturing technology—optics, for example, costs less than before, and lasts longer. The second obstacle (part [ii]) is the more challenging concern, as it must be rigorously addressed if the use of the photons is to be optimized for the intended purpose. For example, if photons are wasted at the source, along the delivery path, or at the target, the economics of the enrichment process will become prohibitive, particularly if the photons are expensive to start with. Another way to express this criterion is in the specific energy consumption of the chemistry process (measured perhaps in moles of product dissociated per joule of laser energy consumed), including all the photon losses from the source to the point where the laser beam is finally discarded. As we will discuss, this economical parameter is closely connected to the control of the *shape* of the laser beam. For now it is enough to note that it is imperative that most of the laser photons be utilized in the separation process, and not lost on optics, or during propagation, or simply as heat in the interaction medium. This is what we refer to as *optimizing the photon utilization* of the process.

All of the interaction processes of laser beams and gas media in multiple-photon dissociation processes are based on nonlinear dependences of the laser beam intensity, with the result that the spatial and temporal distribution of the laser beam is of the utmost importance. Assume for the moment that we have applied our minds to the losses along the delivery path, and have come up with a suitably efficient

delivery system, with optical components chosen to minimize the energy loss from the source to target. In our case, the target would be a reactor chamber where the photons interact with the molecules to be dissociated. Also assume that we have chosen the most efficient lasers possible for the task. That leaves only the reactor itself to consider. Invariably the reactor geometry is fixed (perhaps for gas handling reasons, or to satisfy gas flow constraints), and so very little leeway exists for reactor changes in order to optimize the use of the photons. Thus, good photon utilization must be achieved by making changes to the beam itself. One parameter to be addressed is the intensity distribution of the laser beam, which we will refer to as the *beam shape*. Without careful attention to the beam shape, the dissociation process becomes uneconomical. At first this would appear to be a relatively easy problem to solve. After all, several beam shaping options have matured to the extent that they could be used in a commercial laser plant. However, long reactor path lengths and multiple beams (often of differing wavelengths) often complicate the problem.

In this chapter, we will introduce some of the important variables in an isotope separation process and show how the beam shape influences the commercial success of the process. Rather than discuss the topic from a general perspective, we will use carbon isotope separation as a case study to illustrate the practical aspects of this application. Carbon isotope separation is topical because of the present and future benefits of monoisotopic carbon. In the medical industry, the ^{13}C isotope is already used as a *tracer* in special compounds, whereas ^{12}C has potentially huge benefits for the semiconductor industry as a solution to the heat removal problem in computer circuitry (isotopically pure diamond has a far greater heat conductivity than conventional diamond). Finally, we offer an up-to-date synopsis of progress in laser-based isotope separation.

7.2 MULTIPLE-PHOTON INFRA-RED EXCITATION

Multiple-photon infra-red (IR) excitation is the absorption of many IR photons by a single molecule; often these photons differ in frequency, requiring various sources to be used in the process. Observation of this phenomenon is only possible with the high-intensity sources typical of lasers. The physical process is well understood: a molecule absorbs light by interaction of its electrical dipole with the oscillating electric field of the source. This causes the molecule to start vibrating: radiant energy has been transformed into vibrational energy. If the molecule were an ideal oscillator, the successive vibrational levels would be equally spaced. However, all real molecules deviate from this, due to the fact that the restoring force drops to zero as the bonds stretch further toward breakage (dissociation). Therefore, all real molecules are anharmonic, which means that the spacing between adjacent vibrational levels decreases (is red shifted) with increasing energy.

The energy of an IR photon is very small, and is much less than the energy required to produce dissociation or even chemical reactions. Typically, between 15 and 65 photons are required to dissociate a stable molecule at room temperature. If the laser frequency is selected so that it matches the frequency difference of the first two vibrational levels of the molecule, then due to the anharmonicity,

it would very soon be out of resonance as the molecule is excited to higher and higher vibrational levels. It therefore seemed improbable that a molecule could be excited via a multiple-photon process—how would the remaining photons be in resonance with the molecule? However, during the 1970s several experiments at the Institute of Spectroscopy in Troitzk [1], and at Los Alamos [2], clearly demonstrated that molecules could be excited via a multiple-photon process under certain conditions.

In multiple-photon processes, a molecule with a vibrational absorption band close to the frequency of the irradiating laser can absorb many photons and dissociate without the aid of collisions. The complete analysis of the multiple-photon effect is a complex theoretical problem. Effects that need to be included in such a model are, among others, anharmonicity, coriolis coupling, octahedral splitting, bandwidth considerations of the laser, absorption in the so-called quasi-continuum as well as the unimolecular dissociation of the excited molecule [1–10].

Multiple-photon excitation of a polyatomic molecule by an intense IR laser beam can be divided into three distinct regimes, as shown diagrammatically in Figure 7.1. The initial process is the resonant excitation of the low-lying vibrational transitions (discrete levels), the second stage consists of stimulated transitions in the vibrational quasi-continuum and, finally, photochemical transformation of the highly excited molecules (above the dissociation limit).

The excitation of the lower vibrational levels is of particular interest in isotope separation since this stage of the process determines the isotope selectivity of the multiple-photon process. A nonselective process would imply that both isotopes have been excited. This could happen if the bandwidth of the source is too large, overlapping with the absorption bands of both isotopes. The excitation of these lower levels is through multistep resonant multiple-photon excitations of successive vibrational levels. Anharmonicity causes a frequency detuning of successive vibrational levels,

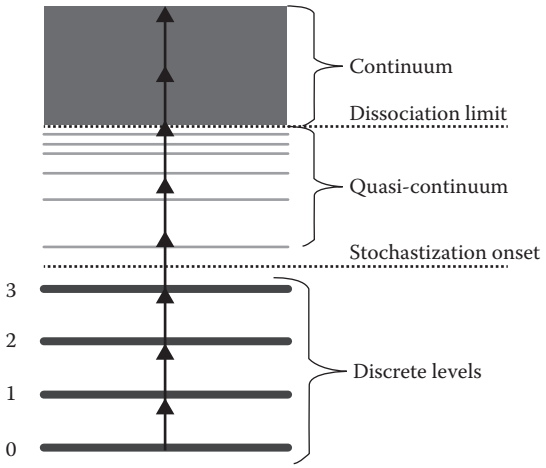

FIGURE 7.1 A simple model of multiple-photon dissociation of a molecule by an IR laser.

which would prevent resonant excitation beyond one or two vibrational levels. This is compensated for by the rotational levels of the molecule, and the anharmonic splitting of the higher vibrational levels. Thus, the same photon frequency can be used to excite the molecule.

The excitation of the lower vibrational levels is a coherent process, and a proper treatment of this subject requires a quantum mechanical model. As the energy of the excited molecule increases, so the density of vibrational states increases sharply. At some level of excitation, a coupling occurs between the overtones of the specific mode that is excited and the background of states.

The Hamiltonian for a molecule near the equilibrium position can be written as follows [3]:

$$H = \sum_{i}^{s} \omega_i \left[(p_i^2/2) + (q_i^2/2) \right] + (1/3) \sum_{i,j,k=1}^{s} \Phi_{ijk} q_i q_j q_k + \cdots \tag{7.1}$$

Where q_i and p_i are the normal momenta and coordinates, respectively.

If the second term in Equation 7.1 is small, then one finds s independent harmonic oscillators, each with its own frequency. This simple picture is a good approximation at low vibrational energies but becomes increasingly inaccurate at higher vibrational energies. As the vibrational energy of the molecule increases, so the higher-order terms in the equation above increase faster than the quadratic ones. The result is that the normal modes start to intermix, giving rise to a change in the intramolecular dynamics. The motion changes from quasi-periodic to stochastic motion. The vibrational energy where this starts to occur is called the stochastization energy. The interested reader is referred to reference [3] for a more detailed explanation of this subject. The result of this stochastization is that the transition spectrum at high excitation energies forms a wide band, which is termed the vibrational quasi-continuum. If the energy of the excitation laser is high enough, then it is possible to excite the molecule to higher energy levels even though the absorption cross section of the transition is small. Owing to anharmonicity, there is a significant red shift with increasing energy. This would mean that as the molecule is excited to higher and higher energy levels, so the optimum excitation frequency would shift to the red. It is for this reason that more than one excitation laser is sometimes used in a multiple-photon excitation process.

Sometimes simple rate equations (also known as kinetic equations) can be used to model the excitation of a molecule. An excitation that can be described using rate equations is sometimes referred to as an *incoherent process*. Usually this approximation can be used when factors are present that would cause the broadening of the spectral lines. For example, if the line width of a transition is much larger than the power broadening introduced by the lasers, then the rate equations give a good approximation. This is the case in the quasi-continuum where the combined absorption band is much larger than the power broadening, and therefore rate equations can be used. Using the transitions in the quasi-continuum, a molecule can accumulate enough energy to exceed the dissociation energy. Owing to the fact that there are

many combinations of vibrational overtones that can participate in the absorption in the quasi-continuum, the energy will be distributed over many vibrational modes.

If the vibrational energy of a molecule exceeds the dissociation threshold, then the molecule can decay spontaneously. The dissociation energy is the breaking energy of the weakest bond. However, the vibrational energy of the molecule will generally be distributed over all the vibrational degrees of freedom of the molecule. Therefore, a fluctuation is required to produce enough energy in the weakest bond for it to be larger than the dissociation energy. This is a statistical process and is analogous to water sloshing around in a bucket; at some stage enough of the energy will be concentrated in a specific degree of freedom (vibrational mode), and a drop of water will fall out of the bucket (the bond will break). The theory that is used to calculate the unimolecular decay is called the Rice–Ramsperger–Kassel–Marcus (RRKM) theory [11].

7.3 ISOTOPE SEPARATION BY LASER DISSOCIATION

Isotope shifts in atomic and molecular spectra are caused by mass differences of the isotopes, nuclear spin, and variations in nuclear volume. Laser isotope separation is based on these isotope shifts. In general, laser isotope separation is divided into the *atomic route* and the *molecular route*. In the *atomic route*, a low pressure metal vapor is generated, and then radiated by tuneable visible lasers. The lasers selectively excite the atoms until the atoms of a given isotope are ionized, thereby producing a selectively ionized species. The isotopes can then be separated electromagnetically.

In the *molecular route*, selective absorption in the infrared is used to excite the vibrational modes of the selected molecule. Since each isotope has a slightly different mode frequency, it is possible to excite selectively by careful choice of laser wavelength and bandwidth. An additional IR or UV laser can then either dissociate the excited molecules or facilitate their participation in a chemical reaction, whereas the unexcited molecule does not dissociate or react. After dissociating, the selected molecule with the required isotope is in a different chemical state to the other isotope(s), and can therefore be separated chemically. Multiple-photon excitation using infrared lasers usually refers to the molecular route, and the isotope separation technique based on this is called *Molecular Laser Isotope Separation* (MLIS).

For example, the enrichment of ^{12}C by the MLIS process involves photons from CO_2 laser systems irradiating Freon gas. Under ideal conditions, the resulting transformation is given by the following reaction:

$$^{13}CHClF_2(g) + {}^{12}CHClF_2(g) \xrightarrow{n \times h\nu} {}^{13}C_2F_4(s) + {}^{12}CHClF_2(g) + \text{by-products} \quad (7.2)$$

In Equation 7.2, the Freon gas ($CHClF_2$) is shown in its two stable forms—that where the carbon atom in the molecule is ^{13}C, and that where it is ^{12}C. The initial ratio of the two gases (right hand side of Equation 7.2) would match the natural isotopic ratio of ^{13}C to ^{12}C; thus, nearly 99% of all the carbon atoms are ^{12}C. This gas is then irradiated by photons ($n \times h\nu$). In this case, the laser photons ($h\nu$) are carefully chosen to interact with only a single vibrational frequency of the selected isotope (^{13}C). Once the selected bond in the ^{13}C Freon molecule is broken (at dissociation), the resulting radical reacts chemically with other radicals to form the solid C_2F_4. In an

ideal scenario, the Freon molecule containing the ^{12}C isotope does not dissociate, and remains in the Freon form (gas phase). Since the ^{12}C isotope is now in the solid phase as C_2F_4, conventional chemical processes can be used to (easily) separate the two isotopes.

In the case of molecules, the isotope shift in the absorption spectrum is a result of the variation in isotope mass. Usually a molecule has a large number of molecular modes. However, only those in which the centre of symmetry of the molecule is disturbed show isotope shifts. This means that for certain normal vibrational modes, the absorption wavelength of two isotopes will be different; this is called the *isotope shift* of the absorption spectrum. The spectrum of a molecule is in reality made up of the superposition of rotational transitions, as well as from contributions arising from vibrational transitions of the thermally populated hot bands. This can be detrimental to isotope selectivity and for this reason the molecules are usually cooled, eliminating the contribution of the hot bands to the spectrum. A widely used method of cooling the gas while still keeping it in the gas phase is to use *flow cooling* through a supersonic de Laval type nozzle, as shown in Figure 7.2.

Lasers required for molecular laser isotope separation face severe technical challenges. Usually the lasers would be used in an industrial plant, which would require continuous operation (24 hours a day, seven days a week). In addition, the throughput in the plant is to a large extent determined by the pulse repetition rate of the lasers. For example, pulse repetition rates needed for a uranium enrichment plant should be approximately 16 kHz. Additional complications are the high pulse energies required for the multiple-photon process (typically 1 J per pulse), and the fact that the lasers sometimes need to be continuously tuneable (which in the case of pulsed CO_2 lasers means that the laser will be operated at a high pressure). Because the isotope shift in the molecule's absorption spectrum is usually rather small, frequency stable, narrow bandwidth operation of the lasers is often required. For the case of UF_6, the absorption band is in the 16 μm wavelength region, but no commercial lasers satisfying all the above requirements are available in this region. Therefore, the *stimulated Raman scattering* process is used to shift the wavelength of a TEA-CO_2 laser from the 10 μm wavelength region to the 16 μm wavelength region. This process usually

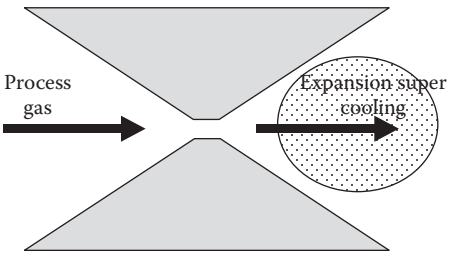

FIGURE 7.2 A de Laval type supersonic expansion nozzle can be used to create super cooled gas. The rapid expansion creates cooled monomers, having a *clean* vibrational spectrum; this is essential for many isotope separation processes. The shaded area indicates the region where the laser beam(s) pass through. The laser beam direction is usually perpendicular to the gas flow.

requires multiple passes through a Herriott type cell, filled with cooled hydrogen. The path length through the Herriott cell can be up to 40 m, implying that good beam quality (for example, Gaussian beams, or beams with beam quality factors of $M^2 \sim 1$) is required to ensure low losses through the system, and good focus ability.

When a techno-economic analysis is performed on the MLIS process, it becomes evident that the cost of photons is of critical importance. In order to obtain an economically feasible plant, it is critical that the photons are utilized efficiently—particularly in the dissociation zone, where the laser beam interacts with the cooled gas, and where the isotope separation actually occurs.

7.4 THE DISSOCIATION ZONE

The dissociation zone is that part of the reactor where the laser beam interacts with the cooled gas, finally causing selective dissociation of the molecule containing the isotope of interest. In the carbon separation process, IR laser beams interact with Freon gas (see Equation 7.2) to dissociate the Freon molecules with the ^{13}C isotope. The amount of dissociation that takes place is measured by the *yield* of the process, whereas the quality of the dissociation (i.e., how selective it is) is measured by the *alpha* of the process. In this section we discuss these concepts, and how beam shapes affect them.

7.4.1 Alpha and Yield

Consider a molecule XY, existing in two states whose composition differs only in that one atom is found in two isotopes: let the molecule with isotope a be XY^a and the other with isotope b be XY^b. Assume that the gas is exposed to radiation that would dissociate the XY^a molecule preferentially. Therefore the concentration of XY^a in the dissociation zone will decrease after irradiation. However, due to the fact that the bandwidth of the laser often overlaps with the absorption bands of both molecules, a fraction of the XY^b molecules will also be dissociated. Assume that the dissociation yield for the two molecules is β_a and β_b, respectively. The selectivity α of the multiple-photon dissociation process is defined as

$$\alpha = \frac{\beta_a}{\beta_b} \tag{7.3}$$

This method of characterizing the selectivity of the process is equivalent to the conventional definition of selectivity [1]. Let $[XY^a]_0$ and $[XY^b]_0$ be the concentration of the molecules before irradiation and $[XY^a]_n$ and $[XY^b]_n$ the concentration of the molecules after irradiation. The conventional definition of selectivity is [1]

$$\alpha = \frac{\dfrac{\left[XY^a\right]_n}{\left[XY^b\right]_n}}{\dfrac{\left[XY^a\right]_0}{\left[XY^b\right]_0}} \tag{7.4}$$

As an example, consider the case of carbon enrichment; the ^{12}C isotope makes up roughly 98.89% of all stable carbon atoms, whereas ^{13}C makes up the remaining 1.11%. Thus initially the ratio of the two isotope fractions is

$$\left(\frac{^{12}C}{^{13}C}\right)_0 = \frac{0.9889}{0.011} = 89.09$$

After some irradiation, with selectivity α, the new ratio (from Equation 7.4) will be given by

$$\frac{^{12}C}{^{13}C} = 89.09\ \alpha.$$

Noting that we can write the percentage ^{12}C in the mix in terms of the fractions as

$$\%^{12}C = 100 \times \frac{^{12}C}{^{12}C + ^{13}C} = \frac{8909\ \alpha\ ^{13}C}{89.09\ \alpha\ ^{13}C + ^{13}C}$$

the purity of the $^{12}_{C}$ isotope (in percentage terms) will be given by

$$\%^{12}C = \frac{8909\ \alpha}{1 + 89.09\ \alpha} \tag{7.5}$$

If there is no separation of the isotopes, then the final isotope ratios will be identical to the initial isotope ratios, since nothing would have changed (no dissociation). From Equations 7.3 and 7.4, we see that this would imply that the numerators and denominators are equal, giving a selectivity parameter of $\alpha = 1$. As the selectivity increases, so the enrichment increases. In the limit of $\alpha \to \infty$, the fraction of ^{12}C increases to 100%, from the initial 98.89% (Equation 7.5).

The two parameters mentioned above, that is, α and β, are of critical importance in the economic consideration of the separation process. Usually α and β follow an inverse relationship: a process with a high yield will have a low selectivity, whereas a process with a high selectivity will have a low yield. Why this is so will become clear later on, when we consider laser beam intensities. For now, it is sufficient to note that in order to achieve a high yield, the laser fluence needs to be high, the result of the high fluence is large power broadening, meaning that the laser spectrum increases, making selective absorption less likely, which in turn would result in a lower selectivity. In contrast, a high selectivity requires very small power broadening, which means low intensities, and consequently lower yields. Once the relationship between yield and alpha is known, a techno-economic analysis can be done to determine the most favorable operating point with regards to laser fluence.

At higher temperatures the higher vibrational modes are also populated, which means that the molecular vibrational spectrum will be scrambled by the overtone transitions. The overtone transitions usually have different isotope shifts as compared to the ground state transition. The result is a decrease in spectroscopic selectivity, which has a negative impact on the economics of the process. The result is

that for many laser isotope separation processes, the process gas is flow cooled in a supersonic expansion nozzle (see Figure 7.2). It is obvious that it is important to irradiate as many of the molecules and to waste as few of the photons as possible. As can be seen from Figure 7.2, the irradiation zone has a very specific geometry. This geometry is determined from the flow conditions and is fixed. It is thus clear that an economical process will require a very specific beam shape in the irradiation zone, and also that this shape must remain constant over the length of the reactor zone.

7.4.2 Process Economics

It was mentioned earlier that there are two important criteria that must be met if an isotope separation process is to be economical: (1) The cost of laser photons or laser energy must be low and (2) the utilization of these photons on an industrial scale must be very good.

This can be written mathematically as follows:

$$\$/\text{kg} = \$/\text{MJ} \times \text{MJ/kg} \tag{7.6}$$

This reads that the cost of producing a kilogram of final product (as measured in dollars per kilogram, $/kg) can be split into the cost per MJ of photons, multiplied by the amount of product (in kg) that those photons produce. The first term is determined by the choice of laser systems used, and relates directly to point (1) our criteria. For most lasers used for isotope enrichment, this value is approximately 100 $/MJ, and, rather surprisingly, does not vary that much from source to source. The second term is a measure of how efficient the entire process is in terms of how many photons are wasted and how many photons are used. Figures 7.3 a and b are simple schematics illustrating the interaction of the laser beam with the gas. In this case, the laser beam volume is described by a pipe, which represents propagation across the chamber used for enrichment. In the case of ^{13}C stripping, the *pipe* diameter might be roughly 6 mm, whereas the length could be in the order of 1 m. In such a volume, approximately 2 μg of product is generated, and only 10% of the photons are used. If the other 90% of the photons are discarded, the second term of the relation in Equation 7.6 can be as high as 500,000. This makes the process commercially unviable. However, if the photons can be used efficiently, which often means passing the beam through the chamber many times, then this cost of producing product in MJ/kg can be made orders of magnitude lower. This is thus the *make or break* step in the entire process; it is this term that plays a significant role in the commercial success of an isotope separation process, and is usually referred to as *photon utilization*.

7.5 BEAM SHAPES AND PHOTON UTILIZATION

All of the interaction processes of laser beams and gas media in multiple-photon dissociation processes are based on nonlinear dependences of the intensity of the laser beam, with the result that the spatial and temporal distribution of the laser beam is of the utmost importance. A common misconception is that the process has a threshold that must be overcome—implying that below a certain laser intensity, no dissociation

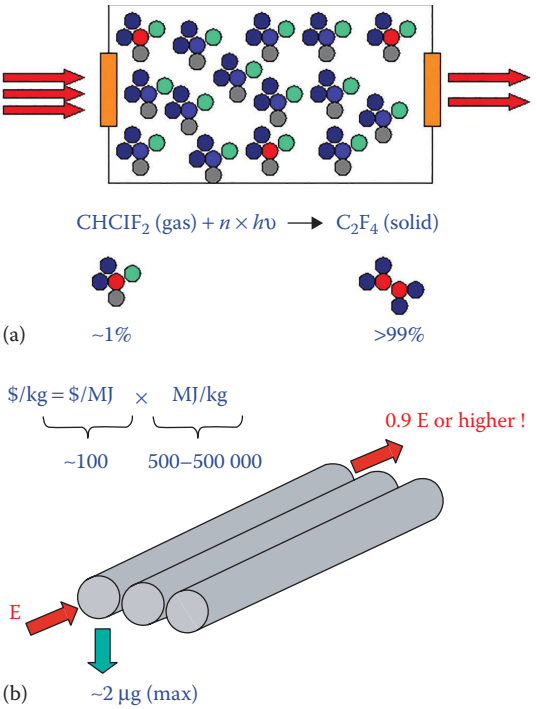

FIGURE 7.3 (a) Energy enters a chamber with a mixture of isotopes. Molecules with one of the isotopes absorb energy, whereas the other molecules do not. After dissociation, the selected isotope is found in a different chemical compound, (b) A simple pipe version of the irradiation process, with each pipe representing the beam irradiation volume of a single pass.

takes place. The multiple-photon process does not have such a threshold; however, at a certain laser intensity the product will be negligible and below the sensitivity of the measurement technique. Thus, for all practical purposes, a *threshold* does exist. In this text, we will refer to threshold with this view in mind.

What happens if the intensity of the laser beam is above or below this threshold? Intensities far below this value will cause negligible dissociation, so the yield will be very small. Intensities far above this will cause power broadening of the molecular spectra, which adversely affects the selectivity of the process, but the yield will be high. In general then, as the intensity of the laser beam increases, so the yield of product increases, but at the expense of selectivity—the product will have a larger mix of isotopes than if the selectivity had been better. Likewise, as the intensity of the laser beam is decreased, so the selectivity increases until a threshold value is reached, below which no (measurable) enrichment takes place due to the accumulative photon energy being lower than the energy needed for dissociation. Thus while the selectivity increases, the yield decreases, and vice versa. One can liken the situation to trying to scoop your favorite sweets from a mixed box, but with different sized scoops. Using a high-intensity laser beam is like using a very large scoop—you maximize the total amount of sweets you get (yield), but at the expense

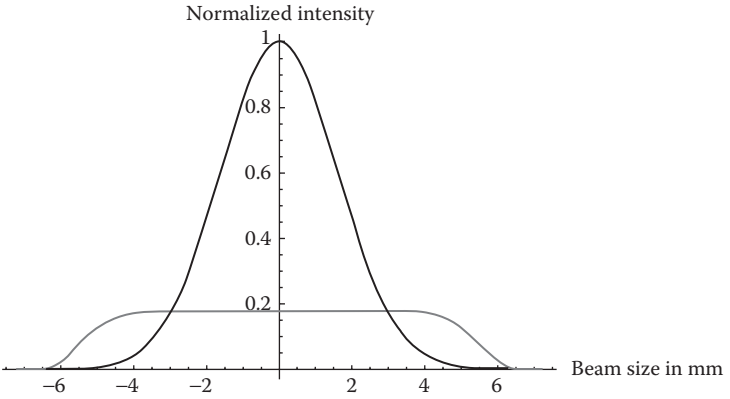

FIGURE 7.4 Example intensity profiles of super-Gaussian and Gaussian beams.

of ensuring that you get only your favorite (selectivity). Conversely, using a small scoop (low-intensity beams) allows you to select your favorites without the unwanted sweets, but the yield in this process is going to be low, that is, fewer of your selected sweets will be gathered in total. Thus, these two parameters need to be balanced, with some of this balancing done by changing the shape of the beam.

When we talk about the *shape* of a laser beam, we are invariably referring to the intensity distribution in the spatial domain. That is to say, if we took a cross section of the beam, the shape would tell us something about how the total energy is distributed across this area. In discussing beam shapes, we will restrict ourselves to two cases: the Gaussian beam and the super-Gaussian beam (see Figure 7.4 for example profiles of each) [12]. Super-Gaussian beams of intensity $I(r)$ and order p are defined as follows:

$$I(r) = I_o \exp\left(-2\left(\frac{r}{\omega}\right)^{2p}\right) \tag{7.7}$$

where:

ω is the beam half width

r is the radial coordinate

The order p indicates the steepness of the intensity drop near $r = \omega$, with increasing values of p indicating flatter intensities with sharper edges. When $p = 1$, the beam is called Gaussian, and follows the standard Gaussian propagation equations. Because the distribution of energy in the two cases (Gaussian and super-Gaussian) is not the same, the peak intensity values will differ, and can be shown to be related by

$$I_s = \frac{p2^{1/p}\omega_g^2 I_g}{2\omega_s^2 \Gamma\left(1/p\right)} \tag{7.8}$$

where the subscripts *s* and *g* refer to the super-Gaussian and Gaussian parameters, respectively. This is an important relationship, because it shows that one requires more energy to get the same peak value in a super-Gaussian beam as in a Gaussian beam.

Gaussian beams are easily generated in resonators that use optical elements with spherical curvatures or even by resonators with diffractive optical elements [13]. Their propagation is well understood, and easily predicted [12]. However, by definition they have an intensity distribution that has a peak value of twice the average (average intensities are calculated by dividing the total power by the beam area, whereas the average fluence is calculated by dividing the total energy by the beam area). This variation in intensity across the beam means that, although some part of the beam will be above the dissociation threshold, other parts will be below the threshold. It also means that the selectivity and yield of the process will vary across the beam area, as well as along the propagation axis—in other words, the selectivity of the process will vary everywhere in the propagation volume (that part of the reactor volume filled by the beam).

Consider the example of enriching carbon using IR beams of both Gaussian and super-Gaussian shape. By ignoring the propagation effects (which will be discussed later), we consider the influence of the intensity distribution only, that is, we assume that the shape remains the same over a certain propagation length. In theory this can be achieved by making the beam size infinitely large, so that the divergence of the beam becomes infinitely small. Before calculating the influence of two different shapes on the final ratio of ^{12}C or ^{13}C that can be generated, we first need to know how the enrichment factor α varies with intensity. Figure 7.5 shows the relationship between the laser beam fluence (energy density) and the resulting enrichment factor α for a given photon wavelength. The measure is given in fluence and not intensity because the time envelop of the pulse was held constant over the experiment, thus only the fluence is needed to characterize the beam's power distribution.

As can be seen from Figure 7.5, as the fluence increases, the selectivity α decreases. At fluences below 800 mJ/cm^2 there is no enrichment due to the fact that the laser beam merely heats up the gas, without actually breaking any bonds. Recall that the Gaussian beam has very low enrichment near its centre, where the fluence is at a peak, and increases toward the edge of the beam area, where the fluence decreases. For this reason, experiments with Gaussian beams are difficult,

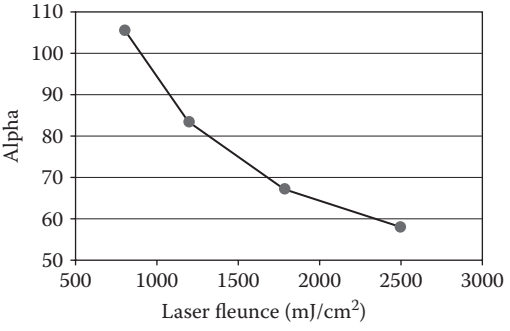

FIGURE 7.5 Alpha versus laser fluence in the isotope separation of carbon.

because the enrichment is an averaging process. By contrast, super-Gaussian beams have the property that the average intensity and the peak intensity have the same value. This means that the entire beam area can be used for dissociation, and that the selectivity and yield will be constant across the beam area. Since all the photons are used equally with this beam shape, very little *averaging* takes place. This makes super-Gaussian beams very attractive for isotope enrichment. However, the propagation effects that were neglected in this discussion play an important role in isotope separation processes. Thus while Gaussian beams can be easily generated and propagated, super-Gaussian beams need to be generated by specially designed optics, whether inside or outside the laser cavity, and have more complicated propagation characteristics as compared to Gaussian beams. These generation and propagation challenges need to be addressed when considering reactor designs.

7.6 REACTOR CONCEPTS

As was just highlighted, propagation effects are very important when considering reactors for isotope separation, and since the propagation of a laser beam is in part determined by the intensity profile of the beam [12], the chosen shape makes a considerable impact on the reactor design. The challenge is to find a beam shape that is optimal, and then design a reactor to hold this shape over an extended distance. Propagation distances in isotope separation processes tend to be long (more than several meters) due to the fact that most media are optically thin (low absorption).

7.6.1 Propagation Issues

The propagation of Gaussian beams can be derived analytically, and is well understood. The divergence of the beam is inversely proportional to the beam size, and together with the wavelength, determines how quickly a given sized Gaussian beam will diverge. The quoted indicator for this is the Rayleigh range, defined as

$$z_r = \frac{\pi\omega_0^2}{M^2\lambda} \tag{7.9}$$

where:

ω_0 is the beam size at the waist (minimum) position
λ is the laser wavelength
M^2 is the beam quality factor

For a perfect Gaussian beam, $M^2 = 1$, although in practice, values of less than 1.2 cannot be easily differentiated from a perfect Gaussian beam. This parameter is a measure of beam quality and increases in value for all shapes other than Gaussian beams (super-Gaussian beams will have $M^2 > 2$).

The propagation of super-Gaussian beams was traditionally achieved by using a suitable input field to the Fresnel diffraction integral, but has since been made easier by the flattened Gaussian beam (FGB) approximation. The propagation of such beams of various classes can now be easily predicted [12].

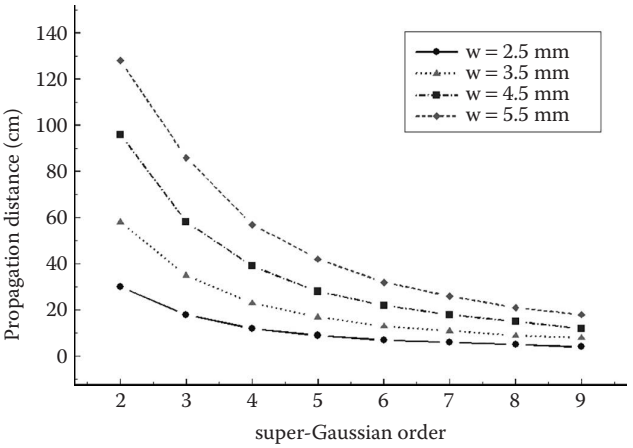

FIGURE 7.6 Maximum propagation distance as a function of super-Gaussian order and starting beam size (w), for a 10% rms change in intensity distribution. The starting field was taken as having a flat wavefront, so that the beam size w is equivalent to the w_0 of Equation 7.9.

The problem in isotope separation is to keep the fluence as constant as possible over the reactor length, while also ensuring that the fluence is above the dissociation limit. Equation 7.9 indicates that beams that are a combination of multiple modes (as a flat-top beam can be seen to be), will diverge faster than single, low order modes, since the M^2 parameter for multimode beams is considerably higher than that of Gaussian beams. Smaller beams will also diverge faster, but the size is limited by the available energy, since the average fluence is calculated by dividing the total beam energy by the beam area. Figure 7.6 shows the distance over which a super-Gaussian beam can be propagated, as a function of both beam size and super-Gaussian order, so that the intensity distribution changes by less than 10% rms. A typical reactor pass length (there will be many passes due to the low absorption) would be in the order of 1 m.

Figure 7.6 then gives an indication of the energy required for a given reactor length and threshold fluence. In order to propagate farther, a larger beam size is required, which in turn requires more energy if the beam is to have the same fluence as the small beam. In most delivery systems, amplification is needed to increase the beam size (while keeping the fluence above the threshold) to a point where there are no major changes in the beam shape over the reactor length. Often it is necessary to have multiple passes through the reactor, due to the fact that the absorption is relatively low through the system. This then complicates the shape-holding criteria—it is simply not good enough to create a given shape, one also must be able to hold (i.e., keep the intensity profile as constant as possible) this shape over an extended distance, which is usually achieved through multiple use of beam shaping optics.

7.6.2 Propagation without Absorption

To consider the influence of propagation effects alone, consider the case of carbon enrichment with a laser system that generates 400 mJ of energy in a Gaussian mode,

and a threshold fluence for suitable dissociation of 1.4 J/cm^2. This means that a Gaussian beam would have to have a beam radius of not more than 3 mm in order for the average fluence of the Gaussian beam to be above the dissociation threshold. For an order 5 super-Gaussian beam, because of the lower peak and average fluences (see Equation 7.8), the beam radius must not increase above 2.39 mm. The shape and size of the beam (with the wavelength) determines the distance that such a field can propagate before the intensity distribution changes (the initial phase of the beam also plays an important role, but for this calculation the phase is taken as flat). To determine how the beam shape changes over a 1 m distance, we propagate the two fields under the scenario of no absorption changes to the beam, that is, we are looking only at intensity changes due to propagation effects. The results are shown in Figures 7.7 and 7.8.

Clearly the benefits of starting with the super-Gaussian shape are diminished in this propagation scenario: the shape does not hold (stay constant to within 10% rms) for long enough to realize the benefits of constant fluence, and therefore constant enrichment and yield. The Gaussian beam on the other hand keeps its shape extremely well over 1 m; Figure 7.7 includes propagation up to 5 m to illustrate the change in shape.

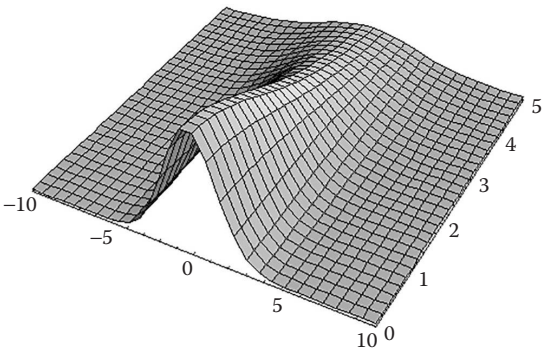

FIGURE 7.7 Intensity changes in a Gaussian beam ($\omega_0 = 3$ mm, $M^2 = 1$, $\lambda = 10.6$ μm) over 5 m.

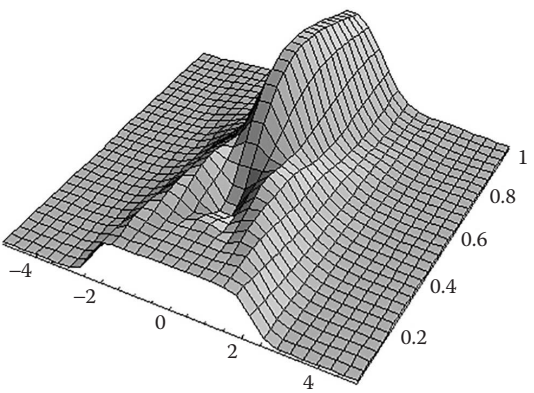

FIGURE 7.8 Intensity changes in a super-Gaussian beam ($\omega_0 = 2.39$ mm, $p = 5$, $\lambda = 10.6$ μm) over 1 m.

The fact that the Gaussian beam holds its shape for longer can be directly related to the fact that this shape has a low divergence for a given field size.

7.6.3 Propagation with Nonlinear Absorption

The important thing to remember about isotope enrichment is that the absorption of the field is nonlinearly dependent on intensity. We now propagate the same fields as in Section 3.2, through the same reactor distance, but take into account the absorption of the gas [14].

The influence of this absorption is determined as follows:

1. The beam, of an initial shape, is entered as a starting field into the Fresnel diffraction integral. An output field is calculated a short distance away.
2. The influence of absorption over this distance is approximated by applying the absorption influences only to the final field. When the distance is very small, this is accurate.
3. The new field is entered into the Fresnel diffraction integral, and the process is repeated.

Because the absorption is a function of intensity, both the absorption and the propagation influence the shape of the beam. The results for the Gaussian and super-Gaussian cases are shown in Figures 7.9 and 7.10, respectively.

The advantage of the super-Gaussian is clear—because of the near constant intensity over most of the beam area, the absorption is the same across this area, thus helping to maintain its shape. Furthermore, because the absorption is larger for high intensities, the formation of peaked shapes, which is characteristic of super-Gaussian propagation, is suppressed. The Gaussian beam clearly shows a flattening of the peak, due to the fact that the absorbance is more in this region than near the edges. At the end of the chamber, the beam is no longer Gaussian, and starts to approximate a low-order super-Gaussian beam. This is a surprising result, because it indicates that by introducing nonlinear

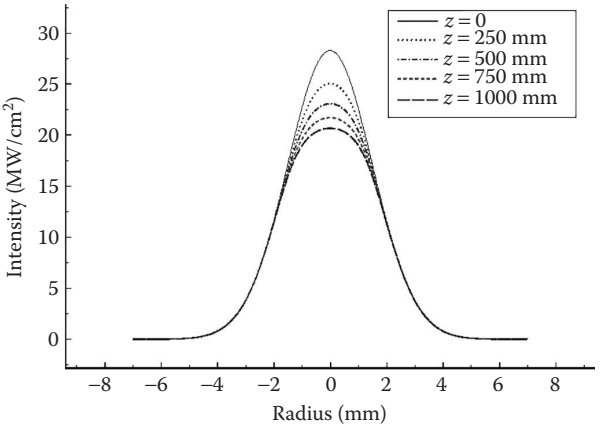

FIGURE 7.9 The Gaussian beam flattens as it propagates through the medium.

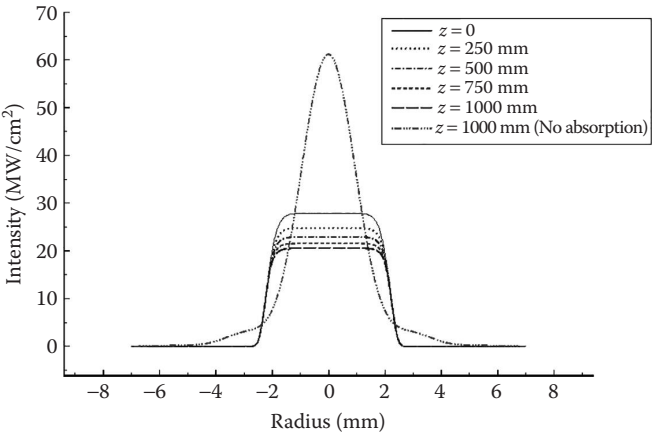

FIGURE 7.10 The super-Gaussian beam holds its shape for longer due to the suppression of intensity spikes.

absorption, the propagation problems mentioned earlier are reduced, as opposed to the expected result that further complexity would simply add to the problem.

The example just given considers a relatively strong absorbing medium, where we have used the absorption of the ^{12}C isotope. If we were instead to dissociate the ^{13}C isotope, the absorption would be correspondingly smaller. In this case, the Gaussian fields would maintain their shape for longer, while the super-Gaussian beam would not. *The choice of beam shape is therefore also influenced by the type of isotope that one chooses to separate.* This result has not been hinted at before in the literature. The choice of isotope, of course, also influences the wavelength that one must irradiate with. Figure 7.11 shows the absorption of ^{12}C in a Freon compound. The absorption is a function of wavelength, as is the propagation.

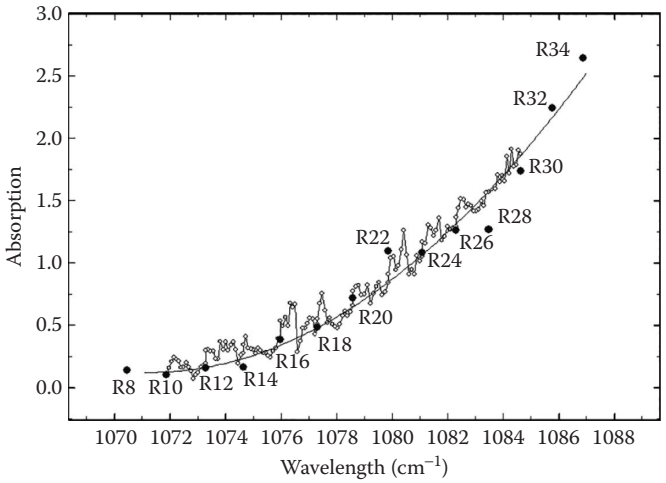

FIGURE 7.11 Multiple-photon absorption spectra of ^{12}C in a Freon compound.

In many cases, the complicating issue in propagation through reactors is the need to propagate several wavelengths together, with very careful spatial and temporal overlap. The major complication is often the beam shapers themselves, which can be wavelength dependent.

7.7 INFLUENCE OF PROPAGATION ON SELECTIVITY

So far we have shown how the intensity of the laser beam affects selectivity and yield. We have also shown how this intensity will change over the length of the reactor by considering propagation of two example fields through the absorbing medium. In the sections that follow, we combine this information to determine the enrichment one can expect for various beam shapes, when taking into account the entire interaction volume.

7.7.1 Experiment

To illustrate the influence of the wavelength and initial beam shape on isotope selectivity, consider the following carbon example:

Dissociation measurements were done on a closed loop system equipped with a 1 m irradiation length nozzle (the total volume of the loop was 16 liters), using a Gaussian beam. The loop was connected to a quadrupole mass spectrometer, allowing online measurement of the enrichment. Batch quantities of process gas were loaded and irradiated, and samples were taken at regular intervals. The laser wavelength was chosen to be in resonance with the ^{13}C isotope. The irradiation therefore was directed at stripping the ^{13}C content from the feed gas. Recall earlier (Equation 7.2) that after dissociation, the ^{13}C isotope is contained in the solid C_2F_4, so *stripping* this from the feed gas simply implies removing the solid product from the flowing gas. The higher the fluence of the laser beam throughout the reactor volume, the quicker the enrichment target of ^{12}C concentration is reached (in this experiment, the target was 99.9%). However, recall that higher fluences resulted in lower selectivity. Once the ^{12}C enrichment of 99.9% was reached, the average bulk ^{13}C enrichment of the dissociated product varied from 20%–60% depending on the specific fluence and wavelength used. Figure 7.12 a shows two different ^{12}C enrichments obtained on the dissociation product by changing the laser fluence, but keeping the wavelength constant. The plot shows how the total enrichment increases with the number of laser pulses used. In an industrial plant, as few pulses as possible would be optimal. Figure 7.12 b shows a plot of absorption peaks obtained by keeping the fluence constant, but varying the laser wavelength from being in resonance with ^{12}C, to between ^{12}C and ^{13}C resonances, to in resonance with ^{13}C. Single-wavelength ^{13}C enrichment of more than 90% has been measured, albeit at low yield.

7.7.2 Numerical Experiment

To consider a slightly different case, we take a 6.5 mm size beam, with 1 J of energy and a pulse width of 80 ns. The beam interacts with the medium, absorbing ^{12}C. Two cross sections are shown for the Gaussian beam, and two for the super-Gaussian

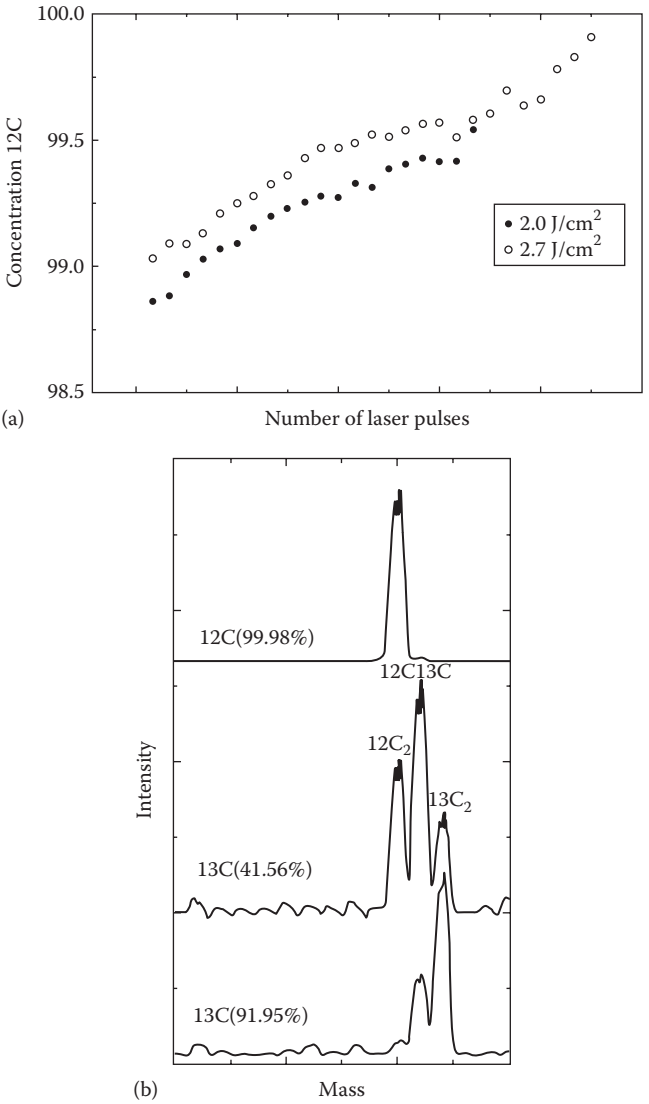

FIGURE 7.12 (a) Enrichment of ^{12}C for two laser fluences, as measured over a period of multiple pulses. The pulse count required for a given enrichment is classified, and so is not shown on the graph and (b) Enrichment of carbon when the laser wavelength is in resonance with ^{12}C (top panel), between resonances (middle panel) and in resonance with ^{13}C (bottom panel). The amplitude of the peaks is a direct indication of concentration of the products formed.

beam. Figure 7.13 shows cross sections that are taken along the propagation axis, in the centre of the beam ($r = 0$ for all z). This monitors the enrichment due to the central part of the beam, which in the case of a Gaussian beam is the peak value of the intensity. Figure 7.14 shows the cross sections in the middle of the reactor, across the beam area ($z/L = 0.5$, for all r).

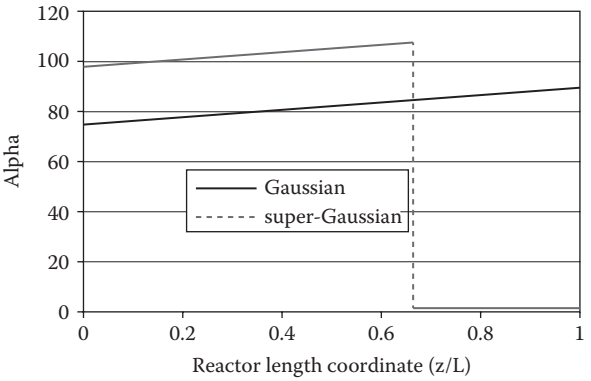

FIGURE 7.13 Alpha along the axis for both a Gaussian and a super-Gaussian beam. The reactor length is normalized to one.

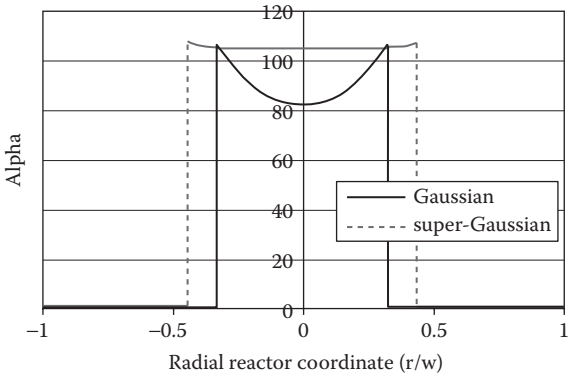

FIGURE 7.14 Alpha across the reactor area, in the centre of the reactor length, for both a Gaussian and a super-Gaussian beam. The reactor radial coordinate is plotted as a normalized value, that is, multiples of the beam size.

In the super-Gaussian case, the fluence along the propagation axis remains nearly constant, as the nonlinear absorption *holds* the shape of the beam. At some point, the intensity of the field is below the threshold, and so no further enrichment takes place. Because the peak intensity is the same as the average, when the intensity falls below the threshold, no further enrichment takes place across the entire field. In contrast, the Gaussian beam shows a steadily increasing selectivity in its central peak. This is because as the absorption decreases, so the alpha increases (recall that lower intensity or fluence gives a better enrichment). Because the peak value is twice the average, at certain stages during the propagation, parts of the beam will not be used.

Figure 7.14 shows the alpha across the beam area in the center of the reactor. Here, the entire super-Gaussian beam area is used, and the alpha is nearly constant

across the beam. The Gaussian case is very different: The central peak intensity of the Gaussian beam results in a lower alpha. As the intensity drops toward the edges of the Gaussian beam, so the alpha increases, until the threshold is reached. Any part of the beam outside this area will not contribute to the enrichment. Thus the area of the reactor used in the Gaussian beam is smaller than that of the super-Gaussian beam.

The influence of the two beam shapes can be summarized as follows: the Gaussian beam results in some of the beam being used all of the time, whereas the super-Gaussian beam results in all of the beam being used some of the time. After adding the contributions across the entire reactor, the Gaussian beam results in an average enrichment factor of $\alpha = 25.3$, whereas the super-Gaussian beam results in an average value of $\alpha = 52.5$. Usually this process would be repeated in multiple stages, with each stage improving the enrichment by this factor. In multiple-stage systems, the final enrichment factor is the product of all the previous enrichment factors. Thus, with an increase by a factor of 2 in the alpha of each stage, after n stages, the enrichment will be higher by approximately a factor of 2^n. This is why the choice of beam shape is so important in isotope separation processes. The number of stages that are required for the same final product purity will be much lower using a super-Gaussian beam than using a Gaussian beam, resulting in huge cost savings.

7.8 BEAM SHAPING CONSIDERATIONS

Traditionally, beam shaping for isotope separation has been achieved with Gaussian beams, using multiple pass cells of the Herriot design [15–17]. This technique has proven inefficient in maintaining a beam with intensity above the dissociation threshold. In recent years there has been much development in both resonator beam shaping [13,18–26] and external cavity beam shaping [27–30] for the creation of flat-top beams. For a detailed discussion, the reader is referred to the references given, or to more general texts on the subject [31].

In making the intracavity versus external shaping choice, careful consideration must be given to the complete beam delivery system. Factors that influence the choice will include the following: the total delivery distance to the irradiation chamber; whether one or multiple wavelengths are used; whether or not amplification systems are used to increase the laser energy; and finally the energy stability of the output beam from the resonator. For example, if a super-Gaussian beam is shaped externally, then the shaping elements can be placed very close to the irradiation chamber. This will make the propagation to the irradiation chamber very easy (Gaussian beam propagation up to the shaping elements), but will be at the expense of beam energy, due to losses on the element, and lower extraction from the resonator and amplifiers. The opposite is true for intracavity shaping–the propagation will be more complex, consisting of relay imaging elements, but the energy extraction from the resonator and amplifiers will be better. As pointed out earlier, the reactor cross section may also have a specific shape due to gas flow considerations. Thus the laser beam area (circular, square, rectangular, etc.) cannot be chosen arbitrarily. To illustrate a typical reactor geometry, consider Figure 7.15.

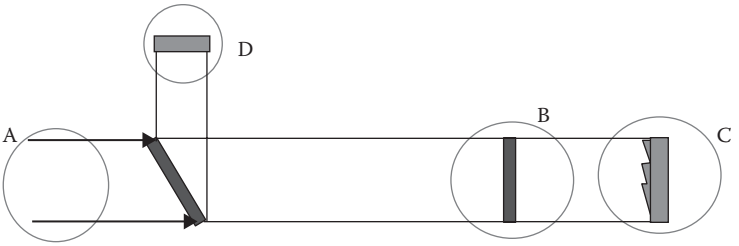

FIGURE 7.15 Example of a reactor model.

In Figure 7.15, the elements A, B, C, and D are as follows:

A. An incoming beam, as formed by one of the *beam shaping* examples. It is assumed to have a super-Gaussian intensity profile, and constant phase. The polarization of the beam is vertical.
B. A quarter wave plate, to induce a λ/4 change in electric field vector. After the second pass, in the return direction, the polarization is changed from vertical to horizontal.
C. Phase conjugate mirror. This diffractive optic takes the phase conjugate of the super-Gaussian field at this point, so that the *reflected* beam de-ripples itself during the return propagation.
D. A flat mirror, which returns the beam. Because the polarization is horizontal, the beam is reflected off the thin film polarizer window immediately before this mirror. The beam at point D is an exact duplicate of the beam at point A.

In the geometry shown in Figure 7.15, a super-Gaussian beam enters the reactor at point A. The polarization allows the beam to pass through the thin film polarizer (TFP) without reflection loss. At point C, diffraction has resulted in intensity variations across the beam, as is evident from the slightly rippled effect seen at some points on the intensity profile of Figure 7.16. In order to minimize this during the rest of the propagation, the beam is reflected off a phase conjugate mirror. After passing through the quarter wave plate (B) for a second time, the polarization ensures that the beam is now reflected off the TFP. The distances are chosen so that after reaching point D, in the absence of absorption, the beam is identical to the starting beam at point A. The return propagation to C is then the same as the initial propagation from A to C. Again the beam passes through the quarter wave plate twice, so that on the final path it is passed back out of the reactor.

The total distance covered is then

$$2\times(\mathrm{A}\rightarrow\mathrm{C})+2\times(\mathrm{D}\rightarrow\mathrm{C}),\ \text{but note that}\ \mathrm{A}\rightarrow\mathrm{C}=\mathrm{D}\rightarrow\mathrm{C}$$

If the reactor length is 1 m, the beam will traverse a distance of 4 m inside the reactor. Figure 7.16 shows the propagation of a super-Gaussian beam through this system. It is important to propagate over as long a distance as possible, since the medium is

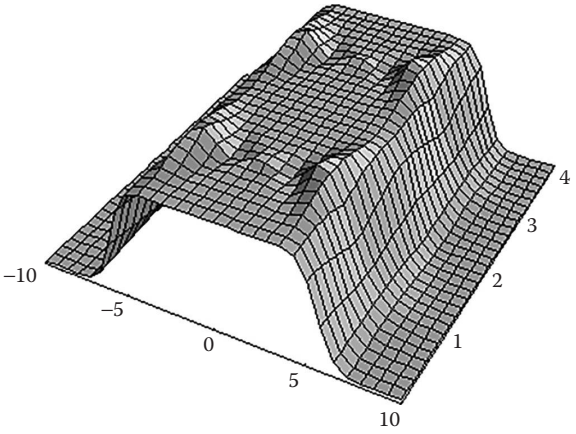

FIGURE 7.16 The intensity plot of a super-Gaussian beam while propagating through the reactor. The total propagation distance is 4 m. At each point during the propagation, the intensity cross section is taken. The reactor has a radius of 10 mm, so cross sections are taken from $r = -10$ to 10.

in general optically thin. If the path length inside the reactor was short, only a small fraction of the total beam energy would be used, and the rest wasted. The photon utilization in this case would be very poor, making the process uneconomical.

It is also obvious from this discussion that the chosen beam shape, and the method to shape it, both have a direct influence on how efficiently the reactor works.

7.9 OUTLOOK AND PROGRESS

In the past decade there has been renewed interest in this field due to advances in beam shaping, laser development, and the economics of certain isotopes [32]. Lithium isotopes have been enriched using a two-step photoionization process with a dye laser [33–35], Gaussian beams of dual wavelength have been used for Barium isotope enrichment [36], all using atomic vapor as the starting phase of the material for enrichment [37]. A major advance in this field has been at the isotope separator on line device (ISOLDE) facility [38]. In this facility, state-of-the-art lasers are used to isotopically enrich a wide variety of elements. The emphasis has been on spatial mode purity and temporal shaping to achieve better enrichment factors. A more recent development has been the approach of coherent-control by optical pulse shaping, usually at time scales faster than the decoherence time of the state under control. This typically makes use of shaped femtosecond pulses [39]. There has also been renewed interest in molecular isotope separation, including carbon [40] and uranium [41], where in the case of the latter a full production plant is presently underway at the General Electric Nuclear Fuel Fabrication Facility (North Carolina, the United States).

Recent advances in laser beam shaping tools are likely to impact on this field. First, the ability to extract maximum energy from the laser cavity and deliver it as a Gaussian mode makes downstream conversion of this mode possible [42].

Second, the multiple wavelengths required for most isotope separation processes can now be shaped with the same element with small perturbations in the size and location of the shaped light, but not in the intensity profile [43]. When these are combined with the new field of temporally shaping ultrafast light, new opportunities arise for highly efficient laser isotope separation.

7.10 CONCLUSIONS

For stable isotope enrichment, good quality beams that hold their shape over an extended distance are required, to ensure effective photon utilization. This is the fundamental difference between beam shaping for isotope separation, and beam shaping for many other applications—in most applications the shape of the beam is important in *one plane only*. For example, in some materials-processing applications, the beam shape at the material surface is very important, but the shape during propagation is not. In isotope separation, however, the beam shape over an extended distance is of importance. Furthermore, propagation through the irradiation chamber shows that the beam shape will change due to nonlinear absorption effects, as well as due to diffraction. In some cases the two work together to hold the beam over longer distances. Because of the intensity dependence of many of the separation parameters, the shape of the beam has a very large influence on the economy of the process, influencing both selectivity and yield as well as overall efficiency.

Today, with the advances in many beam shaping techniques, it is possible to efficiently generate laser beams with intensity profiles of any shape and size. It is this that gives renewed hope to isotope separation by laser-based systems.

ACKNOWLEDGMENTS

I thank posthumously Dr. Lourens Botha for his contribution to this chapter. He was always an enthusiastic supporter of laser isotope enrichment and would be delighted to see it realized one day. I also acknowledge useful data provided by my erstwhile colleagues at Klydon (Pty) Ltd., where isotope separation research continues.

REFERENCES

1. Bagratashvili, V. N., Letokhov, V. S., and Makarov, A. A., Ryabov, E. A., *Multiple Photon Infrared Laser Photophysics and Photochemistry*, Harwood Academic Publishers, Switzerland, 1984.
2. Jensen, R. J., Judd, O. P., and Sullivan, J. A., Separating isotopes with lasers, *Los Alamos Sci*., 3(1), 2–33, 1982.
3. Letokhov, V. S., *Laser Spectroscopy of Highly Vibrationally Excited Molecules*, Adam Hilger, Bristol, 1989.
4. Shen, Y. R., *The Principles of Non-linear Optics*, John Wiley & Son, New York, 1984.
5. Loudon, R., *The Quantum Theory of Light*, 2nd edn., Oxford Science Publications, Oxford, 1983.
6. Shore, B. W., *The Theory of Coherent Atomic Excitation*, John Wiley & Sons, New York, 1989.
7. Suzuki, M. et al., Selective excitation of branched vibrational ladder in uranium hexafluoride laser isotope separation, *J. Nucl. Sci. Technology*, 31, 293, 1994.

8. Larsen, D., Frequency dependence of the dissociation of polyatomic molecules by radiation, *Opt. Comm*., 19(3), 404, 1976.
9. Bloembergen, N., Comments on the dissociation of polyatomic molecules by intense 10.6 μm radiation, *Opt. Comm*., 15(3), 416–418, 1975.
10. Botha, L. R. et al., Continuously tuneable CO_2 MOPA chain for a molecular laser isotope separation pilot plant, *Opt. Eng*., 33(9), 2687–2691, 1994.
11. Frost, W., *Theory of Unimolecular Reactions*, Academic Press, New York, 1973.
12. Forbes, A., *Laser Beam Propagation: Generation and Propagation of Customised Light*, CRC Press Taylor and Francis Group, Boca Raton, FL, 2014.
13. Litvin, I. A., and Forbes, A., Gaussian mode selection with intracavity diffractive optics, *Opt. Lett*. 34, 2991–2993, 2009.
14. Forbes, A., Laser beam propagation in a non-linearly absorbing media, *Proc. SPIE 6290*, 629003, 2006.
15. Fub, W. et al., IR Multiphoton absorption and isotopically selective dissociation of $CHClF_2$ in a Herriot multipass cell, *Z. Phys*., D29, 291–298, 1994.
16. Kojima, H., Uchida, K., Takagi, Y., A Waveguide reactor for IR multiphoton dissociation and its application to ^{13}C laser isotope separation, *Appl. Phys*., B41, 43–48, 1986.
17. Gothel, J., Ivanenko, M., Hering, P., Fub, W., and Kompa, K. L., Macroscopic enrichment of ^{12}C by a high-power mechanically Q-switched CO_2 laser, *Appl. Phys*., B62, 329–332, 1996.
18. Belanger, P. A., and Pare, C., Optical resonators using graded-phase mirrors, *Opt. Lett*., 16, 1057–1059, 1991.
19. Pare, C., and Belanger, P. A., Custom laser resonators using graded-phase mirrors, *IEEE J. Quant. Electron*., 28, 355–362, 1992.
20. Naidoo, D. et al., Transverse mode selection in a monolithic microchip laser, *Opt. Commun*., 284, 5475–5479, 2011.
21. Ngcobo, S., Litvin, I. A., Burger, L., and Forbes, A., A digital laser for on-demand laser modes, *Nat. Commun*., 4, 2289, 2013.
22. Ngcobo, S., Ait-Ameur, K., Litvin, I. A., Hasnaoui, A., and Forbes, A., Tuneable Gaussian to flat-top resonator by amplitude beam shaping, *Opt. Express*, 21, 21113–21118, 2013.
23. Hocke, R., CO_2 Slab Laser with a Variable Reflectivity Grating (VRG) as a Lineselective Element, *Proc. SPIE*, 4184, 427–430, 2000.
24. Leger, J. R., Chen, D., and Wang, Z., Diffractive optical element for mode shaping of a Nd:YAG laser, *Opt. Lett*., 19, 108–110, 1994.
25. Zeitner, U. D., Wyrowski, F., and Zellmer, H., External design freedom for optimization of resonator originated beam shaping, *IEEE J. Quant. Electron*., 36, 1105–1109, 2000.
26. Zeitner, U. D., Aagedal, H., and Wyrowski, F., Comparison of resonator-originated and external beam shaping, *Appl. Opt*., 38, 980–986, 1999.
27. Hoffnagle, J. A., and Jefferson, C. M., Design and performance of a refractive optical system that converts a Gaussian to a flattop beam, *Appl. Opt*., 39, 5488–5499, 2000.
28. Dickey, F. M., and Holswade, S. C., Gaussian laser beam profile shaping, *Opt. Eng*., 35, 3285–3295, 1996.
29. Arrizon, V., Optimum on-axis computer generated holograms encoded into low-resolution phase-modulation devices, *Opt. Lett*., 28, 2521–2523, 2003.
30. Hendriks, A., Naidoo, D., Roux, F. S., Lopez-Mariscal, C., and Forbes, A., The generation of flat-top beams by complex amplitude modulation with a phase-only spatial light modulator, *Proc. SPIE*, 8490, 849006, 2012.
31. Dickey, F. M., and Holswade, S. C., in *Gaussian Beam Shaping: Diffraction Theory and Design, Laser Beam Shaping—Theory and Techniques*, ed. Dickey, F. M., pp. 151–194, Taylor and Francis Group, Boca Raton, FL, 2014.

32. Forbes, A., Strydom, H. J., Botha, L. R., and Ronander, E., Beam delivery for stable isotope separation, *Proc. SPIE*, 4770, 13–27, 2002.
33. Saleem, M., Hussian, S., Rafiq, M., and Baig, M. A., Laser isotope separation of lithium by two-step photonionization, *J. Appl. Phys.*, 100, 053111, 2006.
34. Saleem, M., Hussian, S., Zia, M. A., and Baig, M. A., An efficient pathway for Li6 isotope enrichment, *Appl. Phys.* B, 87, 723–726, 2007.
35. Olivares, I. E., Selective laser excitation in litium, *Opt. J.*, 1, 7–12, 2007.
36. Jana, B., Majumder, A., Kathar, P. T., Das, A. K., and Mago, V. K., Ionization yield of two-step photoionization process in an optically thick atomic medium of barium, *Appl. Phys.* B, 102, 841–849, 2011.
37. Bokhan, P. A. et al., *Laser Isotope Separation in Atomic Vapor*, Wliey-VCH, Wienheim, Germany, 2006.
38. Fedosseev, V. N. et al., Upgrade of the resonance ionization laser ion source at ISOLDE on-line isotope separation facility: new lasers and new ion beams, *Rev. Sci. Instrum.*, 83, 02A903, 2012.
39. Goswami, D., Optical pulse shaping approaches to coherent control, *Phys. Rep.*, 374, 385–481, 2003.
40. Dong, M., Mao, X., Gonzalez, J. J., Lu, J., and Russo, R. E., Carbon isotope separation and molecular formation in laser-induced plasmas by laser ablation molecular isotope spectrometry, *Anal. Chem.*, 85, 2899–2906, 2013.
41. Weinberger, S., Laser plant offers cheap way to make nuclear fuel, *Nature*, 487, 16, 2012.
42. Litvin, I. A., and Forbes, A., Resonator with intracavity transformation of a Gaussian into a top-hat beam, patent 13/266,078, 2011.
43. Forbes, A., Dickey, F., DeGama, M. and du Plessis, A., Wavelength tunable laser beam shaping, *Opt. Lett.*, 37, 49–51, 2012.